

# Journal of Materials Chemistry A

Accepted Manuscript



This is an *Accepted Manuscript*, which has been through the Royal Society of Chemistry peer review process and has been accepted for publication.

*Accepted Manuscripts* are published online shortly after acceptance, before technical editing, formatting and proof reading. Using this free service, authors can make their results available to the community, in citable form, before we publish the edited article. We will replace this *Accepted Manuscript* with the edited and formatted *Advance Article* as soon as it is available.

You can find more information about *Accepted Manuscripts* in the [Information for Authors](#).

Please note that technical editing may introduce minor changes to the text and/or graphics, which may alter content. The journal's standard [Terms & Conditions](#) and the [Ethical guidelines](#) still apply. In no event shall the Royal Society of Chemistry be held responsible for any errors or omissions in this *Accepted Manuscript* or any consequences arising from the use of any information it contains.

## Direct, single-step synthesis of hierarchical zeolites without secondary templating†

Cite this: DOI: 10.1039/x0xx00000x

Zhuopeng Wang,<sup>‡a</sup> Chao Li,<sup>‡ab</sup> Hong Je Cho,<sup>a</sup> Shih-Chieh Kung,<sup>c</sup> Mark A. Snyder<sup>c</sup> and Wei Fan<sup>\*a</sup>Received 00th January 2012,  
Accepted 00th January 2012

DOI: 10.1039/x0xx00000x

www.rsc.org/

Hierarchical ZSM-5 was directly synthesized by controlling the nucleation, growth and template-free self-assembly of zeolite precursors formed in the initial stage of the zeolite crystallization process. The facile synthesis results in spherical particles primarily composed of a micro-mesoporous core of aggregated 30-50 nm MFI nanocrystals, and a thin crystalline shell. MFI nanocrystal assembly coupled with a possible dissolution-crystallization mechanism results in a template-free route to broadly distributed mesopores and, thereby, a ca. 25 nm diffusion length in a micrometer-sized particle. The materials exhibit enhanced mass transport and superior catalytic activity for bulky molecules.

## Introduction

Synthesis of hierarchical zeolites with dual micro/mesoporosity is a proven strategy to alleviate diffusion limitations in zeolite catalysts.<sup>1-3</sup> The presence of mesopores in zeolite catalysts can enhance mass transport and reduce the residence time of molecules, therefore significantly improving both catalytic activity and lifetime of zeolite catalysts.<sup>4</sup> In general, methods for introducing mesopores in zeolites include the post-synthetic modification of zeolites (top-down) and self-assembly by templating methods (bottom-up).<sup>5-7</sup> Desilication and dealumination by steaming or acid/base-leaching are typical examples for the top-down methods.<sup>8-11</sup> In these multi-step methods, mesoporosity is generated within pre-fabricated microporous zeolites by partially dissolving framework Si or Al atoms. On the other hand, the bottom-up strategy offers an opportunity to generate controllable mesopores in zeolites via tailoring crystallization parameters and/or employing pore-forming templates. Recently, numerous attempts have been made to control the mesoporosity of hierarchical zeolites by templating methods. Several hierarchical zeolites have been synthesized using sacrificial templates such as surfactants,<sup>12</sup>

mesoporous carbons<sup>13-16</sup> and amphiphilic organosilanes.<sup>17</sup> A breakthrough in this approach was made by Ryoo and co-workers.<sup>18, 19</sup> In their method, hierarchical zeolites with tunable mesopores or single-unit-cell nanosheets were synthesized using appropriately designed surfactants containing two functional groups for directing micropore and mesopore structure, respectively. In contrast to the use of elaborately synthesized surfactants, Tsapatsis and co-workers have developed a facile way to synthesize self-pillared single-unit-cell zeolites using conventional structure-directing agents.<sup>20</sup> Although significant developments have been achieved in the synthesis of hierarchical zeolites, secondary templates are often indispensable for controlling the mesoporous structure of hierarchical zeolites. One-step, facile and low-cost synthesis of hierarchical zeolites without the need for secondary templates or post-synthetic treatment is highly desired. A few examples of such strategy have been realized, including mesoporous ZSM-5 made by promoting nucleation,<sup>21</sup> mesoporous ZSM-5 single crystals made by tuning the synthesis parameters,<sup>22, 23</sup> seed-induced synthesis of mesoporous ZSM-5 aggregates,<sup>24</sup> and one-pot synthesis of hierarchical zeolite beta by steam-assistant crystallization.<sup>25</sup>

In order to circumvent the need for secondary templates to realize a one-step, bottom-up approach to zeolites with dramatically reduced diffusion lengths, insight into and control over zeolite crystallization is critical. The zeolite crystallization process under hydrothermal conditions has been extensively studied. Precursor nanoparticles in the range of 2-20 nm were often observed in the early stage of the zeolite crystallization process.<sup>26-28</sup> The precursor nanoparticles were shown to evolve to zeolite nuclei by a series of reactions with the surrounding synthesis sol.<sup>26</sup> They can also further support crystal growth by providing growth nutrients, and affect the final morphology of the formed zeolites.<sup>29, 30</sup> Inspired by these

<sup>a</sup> Department of Chemical Engineering, University of Massachusetts Amherst, MA 01003, USA. E-mail: wfan@ecs.umass.edu; Fax: 413-545-1647; Tel: 413-545-1750

<sup>b</sup> School of Chemistry and Chemical Engineering, South China University of Technology, Guangzhou, 510640, China

<sup>c</sup> Department of Chemical and Biomolecular Engineering, Lehigh University, Bethlehem PA 18015, USA

† Electronic Supplementary Information (ESI) available: [details of any supplementary information available should be included here]. See DOI: 10.1039/b000000x/

‡ These authors contributed equally to this work.

observations, an alternative method for the synthesis of hierarchical zeolites has been developed.<sup>12, 31</sup> In this method mesoporous structure was generated by precisely controlling the assembly of the precursor nanoparticles, and thereby the interstitial space therein, using surfactants as secondary templates. Hierarchical zeolites were subsequently formed by converting the assembled nanoparticles into zeolite crystals without interfering with the preformed, surfactant-induced mesoporosity. Early studies on this approach were focused on using surfactants to manipulate the assembly of the precursor nanoparticles and their crystallization process. However, the use of surfactants not only increases the complexity and cost, but also often results in a mixture of amorphous mesoporous silica and bulky zeolite.

In this work, we report a facile method for direct, one-step synthesis of hierarchical zeolites that circumvents the need for secondary templating and yields a remarkably small diffusion length (ca. 25 nm) within sub-micrometer spherical zeolite particles. In this method, the mesoporosity in the ZSM-5 crystals derives from controlling the formation and template-free self-assembly of zeolite precursor nanoparticles, formed during the initial stage of the crystallization process. The largely reduced diffusion length endows the hierarchical ZSM-5 with superior catalytic activity for reactions involving bulky molecules. This attractive approach for synthesizing hierarchical ZSM-5 catalysts provides an alternative to more costly and complex 'bottom-up' and 'top-down' approaches, and holds potential for even broader applicability to a wide range of zeolites and even other porous materials.

## Experimental section

### Synthesis of hierarchical ZSM-5 with different Si/Al ratio

The synthesis was started from a clear synthesis sol prepared by mixing the silicon source (Ludox HS-40, Sigma Aldrich), aluminum source (aluminum isopropoxide, 98%, Sigma Aldrich), NaOH and tetrapropylammonium hydroxide (TPAOH, 1 M, Sigma Aldrich) with a composition of  $\text{SiO}_2:0.25\text{TPAOH}:x\text{Al}_2\text{O}_3:0.014\text{Na}_2\text{O}:16.44\text{H}_2\text{O}$ . Target Si/Al ratios of 80, 50, and 30 correspond to  $x = 0.00625$ , 0.01 and 0.0167, respectively. Hydrothermal treatment was carried out in a Teflon-lined autoclave at 135 °C for up to 4 days with a rotation of 3 rpm.

Typically, for the synthesis of hierarchical ZSM-5 with Si/Al = 30, 0.233 mL of 10 M NaOH solution and 0.1631 g of distilled water were added to 20.806 mL of 1 M TPAOH solution (Sigma Aldrich). Subsequently, 12.5 g of Ludox HS-40 was added dropwise to the mixture. A transparent solution was obtained after stirring the mixture for 1 h. Thereafter, 0.5663 g of aluminum isopropoxide was added and completely dissolved into the solution by stirring for 30 min. Hydrothermal synthesis was performed in a Teflon-lined autoclave at 135 °C with a rotation of 3 rpm. The obtained product was thoroughly washed by filtration with distilled water, followed by drying at 100 °C for overnight and calcination in a furnace set at 550 °C for 12 h in air. Ion exchange of the products with 1 M aqueous solution of  $\text{NH}_4\text{NO}_3$  at 80 °C for 2 h was repeated three times. The final products were converted to H-form by calcination at 550 °C for 8 h.

For the experiments with different aging times, prior to hydrothermal treatment the synthesis solutions were aged from 1 to 3 days at room temperature under static conditions. For the syntheses with different NaOH concentration, the amounts of NaOH were adjusted to 1/2, 1/10 and 1/50 of the molar ratio of NaOH described above (hereafter denoted as 1 NaOH, 1/2 NaOH, 1/10 NaOH and 1/50 NaOH with a descending order of NaOH concentration). Detailed synthesis conditions are listed in Table S1.

### Zeolite precursor retrieval

Precursor particles were extracted from the synthesis sol after 3 h of hydrothermal treatment according to the method reported previously.<sup>28, 32</sup> A saturated solution of cetyltrimethylammonium bromide (CTMABr, Aldrich) in ethanol was added dropwise into the synthesis solutions with stirring until a white precipitate formed. The solid was washed with ethanol and dried in a vacuum oven at room temperature for 24 h. For the dry gel conversion, the extracted sample (ca. 1 g) was ground into powder and put into a Teflon-lined stainless steel autoclave with a cup volume of ca. 50 mL. A portion of 0.5 mL of distilled water was added into the autoclave in a separate Teflon cup to avoid direct contact between the dry gel and water. The autoclave was then placed in an oven preheated to 135 °C for 5 d. The as-made sample was washed by filtration with 1 L of distilled water and dried at 100 °C overnight. The sample was calcined at 550 °C for 6 h before other characterization.

### Characterization

Scanning electron microscopy (SEM) images were collected on an FEI-Magellan 400, equipped with a field-emission gun operated at 3.0 kV after the samples were coated with Pt. Transmission electron microscopy (TEM) investigation was conducted on an FEI Tecnai G2 F30 transmission electron microscope operating at 300 kV. Thin section samples for the TEM observation were prepared by embedding particles in epoxy resin (Araldite, Embed-812), followed by sectioning with a Leica EM UC6 microtome. The obtained ~50 nm thin sections were mounted on a grid (400 mesh, Cu, Ted Pella) for TEM observation.  $\text{N}_2$  and Ar adsorption/desorption isotherms were measured on an Autosorb®-iQ system (Quantachrome) at 77 K and 87 K, respectively. Pore size distribution and cumulative adsorbed volume were calculated by using NLDFT (non-local density functional theory) adsorption model which describes Ar adsorbed onto silica with cylindrical pores at 87 K (AsiQwin 1.02, Quantachrome). Powder X-ray diffraction (XRD) patterns were collected on a PANalytical X'Pert diffractometer using  $\text{Cu K}\alpha$  radiation. Data was collected in  $2\theta$  range from 4° to 40° with a step size of 0.02° and a step time of 1 s. Elemental analyses were performed on an inductively coupled plasma-optical emission spectrometer (iCap 6500 dual view, Thermo Scientific). Pyridine FT-IR study was performed on EQUINOX 55 (Bruker) with an MCT detector. The sample was degassed at 550 °C for 1 h by flowing He in order to remove adsorbed water. Afterwards, small aliquots of pyridine were exposed to the sample at 120 °C for 15 min. Prior to the FT-IR measurement, the weakly adsorbed pyridine molecules were removed under a He flow at 250 °C for 1 h. The spectra were then collected at 120 °C.

### Determination of acid sites

Isopropylamine temperature program decomposition (IPA-TPD) was carried out on a TA instrument Q500 following a procedure developed by Gorte et al.<sup>33,34</sup> 0.015 g of catalyst was first pretreated at 550 °C for 1 h under a He flow with a rate of 100 cm<sup>3</sup>/min to remove the water and other impurities adsorbed on the catalyst surface. After cooling down to 120 °C, IPA was dosed into the system. When the sample was saturated with IPA, the gas flow was switched to He. Oven temperature was then increased to 700 °C with a ramping rate of 10 °C/min. The decomposition of IPA into ammine and propylene occurred between 300 °C and 400 °C. 2,4,6-trimethylpyridine (collidine) TPD measurement was carried out in a similar way with IPA-TPD. The weight loss from 300 °C and 400 °C was used to determine the acid sites on the external surface of the catalyst.

### Zero length column chromatography (ZLC) measurement

The ZLC setup used in this work was described in our previous studies.<sup>35,36</sup> All gas flow rates were controlled with Brooks 5850E mass flow controllers. Partial pressure of cyclohexane (>99%, Acros Organics) was maintained by equilibrating a low flow helium stream with a liquid cyclohexane reservoir at 283 K. Prior to diffusion measurements, the crystals were preheated at 523 K for 8 h under helium flow of 50 mL/min to remove physically adsorbed water. Cyclohexane was carried by low-flow helium (2.5 mL/min) from the adsorbate tank and further diluted with helium in the main stream (100 mL/min).

Adsorption of cyclohexane (~2 torr) in the zeolite samples begins when a valve is actuated to allow the premixed stream of helium and cyclohexane to flow over the sample chamber, and the uptake is monitored online. Care was taken to ensure the equilibration time was greater than  $0.416 R^2/D_{eff}$  to eliminate partial saturation effects<sup>37</sup>, where  $D_{eff}$  is the effective diffusivity of adsorbate in the crystal, and  $R$  is the radius of the crystals. After adsorption reached equilibrium, the valve was switched back to pure helium flow. Flow rates of 25-100 mL/min were used with hierarchical ZSM-5 (Si/Al = 30) at 90 °C to examine whether desorption process was controlled by the molecular diffusion in micropores, and a purge flow rate of 50 mL/min for helium was selected for the zeolite samples. Desorption of adsorbate from the zeolite samples was monitored by measuring the concentration of adsorbate in helium flow with a flame ionization detector (FID). The data was analyzed using linear ZLC analysis of desorption curves developed by Eic and Ruthven.<sup>38</sup> Detailed method can be found from the Electronic supplementary information (ESI).

### Catalytic reaction

The catalytic performance of synthesized catalysts was tested with a benzyl alcohol self-etherification reaction. The reaction was carried out by following the experimental procedures described by Tsapatsis et al.<sup>20</sup> Typically, 0.117 g of zeolite catalyst was added to 15 mL of mesitylene. All zeolite catalysts were activated at 550 °C in a muffle furnace for 4 h before use. 0.051 mL 2,6-di-tert-butylpyridine (DTBP) was added to poison the acid sites on the external surface of catalysts. The reaction mixture was refluxed for 2.5 h at 70 °C with

stirring before 0.25 mL of benzyl alcohol was added. Reaction time was defined as the time after addition of benzyl alcohol. Liquid samples were withdrawn at regular intervals and analyzed by a gas chromatograph (Agilent HP-6890 GC) equipped with a methylsiloxane capillary column (HP-1, 50.0 m × 320 μm × 0.52 μm) connected to a FID. The calculation of catalyst effectiveness factor ( $\eta$ ) and Thiele modulus ( $\phi$ ) are list in ESI.

## Results and discussion

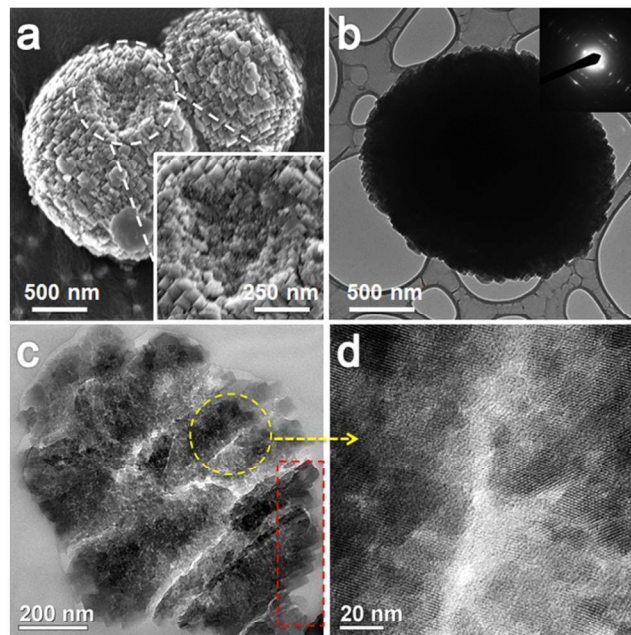


**Fig. 1.** Electron micrographs of hierarchical ZSM-5 (Si/Al = 30) synthesized in 24 h: a) SEM image, b) TEM image and SAED pattern(inset), c) TEM image of the cross-section of an entire particle (red cycle: crystals grown on the shell), d) enlarged image of the core of the particle shown in c).

Clear solution systems are frequently used to synthesize nanosized zeolites.<sup>39</sup> With clear solution method, it is relatively easy to control both nucleation and crystal growth processes of zeolites. Therefore it provides us opportunities to manipulate precursor particles and nanocrystals to assemble into hierarchical structures. In this work, the synthesis of hierarchical ZSM-5 started from a clear synthesis sol with a composition of SiO<sub>2</sub>: 0.25TPAOH: 0.0167Al<sub>2</sub>O<sub>3</sub>: 0.014Na<sub>2</sub>O: 16.44H<sub>2</sub>O (Si/Al=30). Instead of TEOS, we chose more active silica sol, Ludox HS 40, as the silica source, differing from other clear solution recipes (Table S2). Hydrothermal treatment was conducted in a Teflon-lined autoclave at 135 °C for up to 4 days with a rotation of 3 rpm.

XRD patterns of the samples (Fig. S1) show the characteristic reflections of the MFI structure without other impurities. SEM images (Fig. 1a and S2) show that the samples with Si/Al = 30 are spherical aggregates. The outer surface is comprised of discrete, stacked crystallites of ca. 50-100 nm in size, some of which bear a typical coffin-shape characteristic of MFI zeolite, indicating that each crystal might be grown from an individual nucleus. The circled area in Fig.1a highlights a part of the aggregate wherein this outer surface is partially removed to reveal an interior of the particle

bearing a distinctly different morphology than the thin shell. Specifically, the magnified view in the inset of Fig. 1a reveals a core that is apparently comprised of aggregated nanoparticles.

As a basis for establishing initial fundamental insight into synthesis-structure relations defining the direct, one-pot route to such hierarchical structures, thin microtomed slices of epoxy-embedded samples were studied by TEM. Fig. 1c shows a representative TEM image of such a cross-section, in which the white slits are believed to be microtome-induced cracks, artefacts commonly observed from such sectioning of micrometer sized zeolites embedded in an epoxy resin. The representative image confirms the existence of a thin (i.e., tens of nanometers) outer coating of the particles, composed of stacked and intergrown zeolite crystals (Fig. 1c, red dashed rectangle), which is consistent with the morphology of the external surface observed by SEM. More importantly, however, it reveals how the majority of the particle is comprised of a core with a distinct nanoparticulate morphology achieved through a direct synthesis route employing no secondary template. HRTEM of a sub-section of the core (Fig. 1d) reveals lattice fringes that indicate that the core nanoparticles, of sizes ranging from 30 nm to 50 nm, are highly crystalline. The selected area electron diffraction (SAED) pattern from a representative aggregate (Fig. 1b) underscores this crystallinity. Moreover, it reveals a surprisingly low degree of polycrystallinity for the full aggregate, suggesting that the aggregate itself is composed of just several larger single crystal domains of slightly different orientation. The nanocrystallite morphology of the core of the particles, bearing a clear network of open interstitial pore space as revealed in Fig. 1d, makes this an especially striking finding. Taken together, the low degree of polycrystallinity and apparent intercalating mesopore topology, provides first insight that the template-free mechanism for formation of the hierarchical zeolite core may involve self-assembly and/or oriented aggregation of pre-formed nano-crystalline zeolite particles.

In an effort to elucidate mechanistic insight into this direct formation of hierarchical ZSM-5, the existence and evolution of mesoporosity and morphology within the hierarchical particles was followed by Ar physisorption, SEM, TEM and XRD. Fig. 2a shows Ar physisorption isotherms collected on the samples with Si/Al = 30 after synthesis times spanning from 18 h to 4 d. The physisorption isotherms in all cases show characteristic micropore filling, as revealed by the sharp increase in volume adsorbed at  $P/P_0 < 0.05$ . The micropore volume clearly indicates that after just 18 h of synthesis, the sample already has a highly crystalline micropore texture that is sustained throughout the duration of the 4 d synthesis, consistent with the corresponding XRD patterns (Fig. S1). SEM (Fig. S3a) and TEM images (Fig. S4a) of the 18 h sample show particles comprised of aggregates of fine nanocrystallites. SAED (Fig. S4a, inset) confirms the crystallinity of these nanocrystallite aggregates, with the specific diffraction revealing a low degree of polycrystallinity consistent with that observed for the full particle. Longer synthesis results in the growth of coarser crystals on the surface, but persistence of the fine nanocrystallite morphology of the core.

In addition to insight into the onset and persistence of microporosity throughout the crystallization process, Ar physisorption (Fig. 2a) also reveals the development of mesoporosity within the structures. Namely, a subtle hysteresis is observed in the case of the sample crystallized for 18 h, a signature of capillary condensation indicative of the untemplated interstitial mesopores intercalating the aggregated nanocrystallites. NLDFT analysis (Fig. 2b) applied to the adsorption branch shows that these mesopores are fairly broadly distributed. Upon increasing the crystallization time, this subtle hysteresis evolves into distinct hysteresis loops. A corresponding shift in the closure of the adsorption and desorption branches to higher relative pressures is indicative of a concomitant increase in the mean mesopore size. This is borne out by the corresponding pore size distributions (Fig. 2b), which also reveal an apparent broadening of the mesopore size (e.g., pore width of 3-5 nm for the 18 h sample and 3-15 nm for the 4 d sample) as a result of the increasing crystallization time rather than any post-synthetic treatment. Accordingly, the total mesopore volume and external surface area of the samples decrease with increasing crystallization time (Table S1). This is likely due to the growth of the primary particles in both the core and shell.

It is known that for the synthesis of MFI zeolites from a TPAOH/SiO<sub>2</sub> system, the introduction of aluminum will slow down the crystal growth rate, which can be further reduced when the concentration of aluminum is increased. This could be due to the relatively low solubility of aluminosilicate gel formed during syntheses, which leads to a longer equilibrium time between the liquid and solid phases compared to a pure silica system.<sup>40</sup> Indeed, in our experiments, we observed that the runs with Si/Al=80 showed the highest crystallization rate and the rate decreased with the decrease of Si/Al ratio. Figure 2c shows the Ar adsorption/desorption isotherms for the samples with Si/Al = 30, 50 and 80. The hysteresis loops in the isotherms became less apparent when the Si/Al ratio of samples increased from 30 to 80. The pore size distributions for the three samples were estimated by NLDFT method as shown in Fig. 2b. The sample with Si/Al = 30 showed a broad pore distribution of 2-11 nm. The other two samples showed a similar pore size distribution, but less amount of mesopore (Table S1).

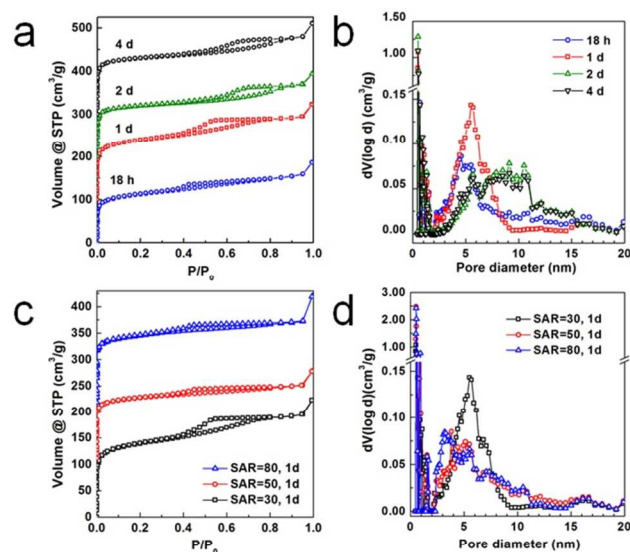


**Fig. 2.** Ar adsorption/desorption a, c) isotherms (shifted 100 cm<sup>3</sup>/g vertically for clarity) and b, d) corresponding NLDFT pore size distribution of samples with different crystallization times and different Si/Al ratios.

As alluded to earlier and discussed in more detail later, zeolite precursor particles appear to play an important role in the direct synthesis of hierarchically porous ZSM-5. It is well-known that the NaOH concentration in the synthesis sol and aging time can affect the stability of the precursor particles and the crystallization rate of zeolites. This raises questions about the robustness of the direct synthesis approach described here to factors like alkali concentration and aging time. Here, we have systematically and independently varied both parameters, controlling NaOH concentration over a wide range spanning from the nominal concentration to a small fraction (1/50) thereof, and studying up to three days of aging. Our study shows that although the crystallization rate is related to the NaOH concentration and aging time, their effects on the mesoporosity of the hierarchical ZSM-5 are not significant as revealed by the relative insensitivity of the nitrogen physisorption (Fig. S7) and corresponding textural properties (Table S1). All samples with different NaOH concentrations exhibit a similar morphology (Fig. S8). It should be noted that the presence of NaOH is crucial for the synthesis. In the case of no NaOH, an amorphous phase was formed even though the synthetic time was extended to 7 d. A plausible explanation is that small  $\text{Na}^+$  ions are much better charge compensators compared with  $\text{TPA}^+$  that can assist the incorporation of aluminum.<sup>41</sup>

In addition, different silica sources were also used in the synthesis. Representative SEM images of the morphology of the derived particles along with powder XRD and nitrogen adsorption isotherms are shown in Fig. S9 for fumed silica and tetraethylorthosilicate (TEOS) silica sources. These data show that in the case of the direct, one-step synthesis technique, use of fumed silica and colloidal silica (Ludox HS-40) results in the formation of hierarchical structures, while only uniform single crystalline ZSM-5 is obtained with TEOS (Fig. S9).

On the basis of these results, the template-free formation of the hierarchical structure likely starts from the aggregation of precursor particles formed in the initial stage of the crystallization process. Subsequent crystallization and Ostwald ripening processes could play important roles in the formation of the highly crystalline

hierarchical ZSM-5 samples. In order to study the precursor particles formed in the early stage of the crystallization process, the solution obtained after 3 h of hydrothermal treatment was observed by TEM and DLS. Uniform spherical nanoparticles with a size of around 30 nm were observed in the synthesis sol (Fig. 3a). The particle size agrees well with the data from DLS measurement as shown in Fig. 3b. To investigate their structure, these particles were extracted from the synthesis sol using an ethanol/surfactant solution according to the method reported previously.<sup>28,32</sup> Two broad peaks centered at  $2\theta$  of ca.  $8^\circ$  and  $23^\circ$  were observed in the XRD pattern of the obtained sample (Fig. 3c). Given that the broad higher angle diffraction is consistent with that of amorphous silica, the peak at  $2\theta$  of  $8^\circ$  is unlikely related to an internal atomic structure of MFI crystals. Instead, it is most likely a feature associated with particles or units with a size of around 1.2 nm as suggested by previous literature.<sup>42</sup> Precursor nanoparticles with longer synthetic time (6 h, 9 h and 13 h) were retrieved and studied as well (Fig. S10 and S11), however, no signature of MFI was observed. Crystalline phase was first detected after 15 h of hydrothermal treatment although the crystallinity is low.

Although no MFI characteristic peaks were observed from XRD, it is worth mentioning that the extracted particles can be further crystallized (Fig. S12) by a dry gel conversion method, implying that these particles may have a certain degree of similarity in composition and structure with the final ZSM-5 crystals. The roles of precursor particles in the crystallization process of zeolites have been demonstrated in several model systems.<sup>43-45</sup> Recently, a mechanism for the early stage of siliceous MFI growth was proposed by Tsapatsis et al.<sup>26, 46</sup> It involves the evolution of precursor nanoparticles to nuclei and crystal growth by the aggregation of a fraction of the evolving nanoparticles. Lobo et al. demonstrated a similar behavior for the precursor particles involved in the formation of Al-containing zeolites.<sup>44, 47</sup> They specifically observed that the incorporation of Al in precursor particles can affect the interparticle repulsion by lowering surface charges, therefore promoting nucleation and the formation of secondary particles. In the present study, it is conceivable that a similar mechanism may drive the aggregation of precursor particles into the nanoparticulate aggregates, observed for the shortest crystallization times studied and persisting as the particle core at longer crystallization times. Moreover, the concentration of Al in the samples might affect the structure and stability of the precursor particles, resulting in the measured sensitivity of sample mesoporosity to Si/Al as previously discussed.

Based on the parametric studies of the synthesis of the hierarchical ZSM-5 herein, characterization of the precursor particles, and analysis of the evolving structure, morphology, and texture as a function of crystallization time, we propose a possible formation scheme as described below and depicted in Scheme 1. Precursor particles with a particle size of around 30 nm are formed during the early stage of the crystallization. These particles may be composed of even smaller nanoparticles as shown by the XRD (Fig. 3c) and suggested by previous literature.<sup>26, 44</sup> The structure of the precursor particles is amorphous at the beginning of the crystallization, but likely evolves to a crystalline structure similar to that of MFI during the course of crystallization. The precursor particles self-assemble to spherical aggregates with a size of around 500 nm, a process that seems to be sensitive to the Si/Al possibly due to its role in modulating surface charge and thereby inter-particle interaction and assembly. The interstitial spacing between the assembled precursor particles forms a 3D-interconnected network of mesopores without

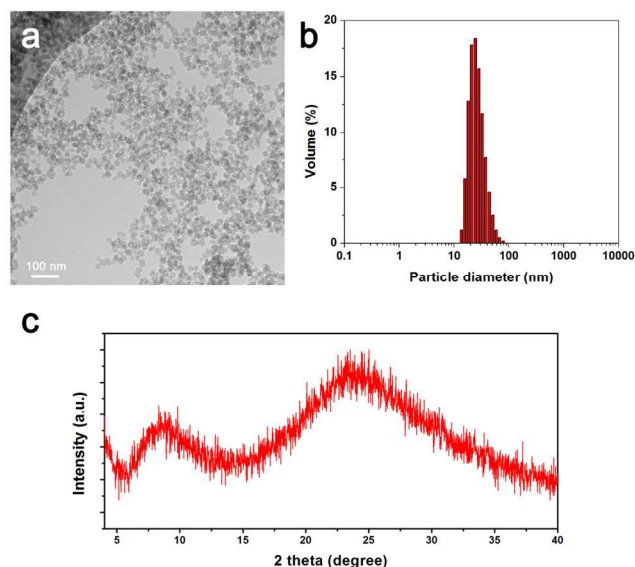
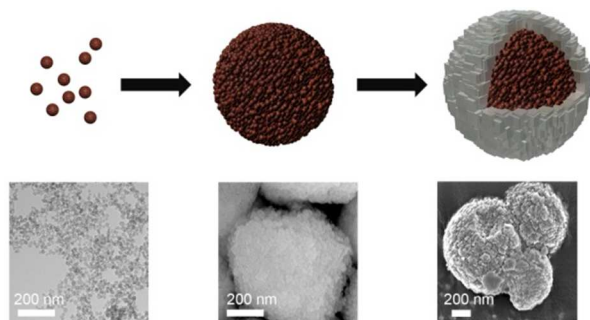


**Fig. 3.** a) TEM image, b) particle size distribution obtained from DLS and c) powder XRD of the particles collected after 3 h of hydrothermal synthesis.

the need for a secondary template. The mesopores are further developed by partial dissolution of precursor nanoparticles in the core region of the aggregates as reflected in the broadening of the mesopore size distribution despite the persistence of crystalline microporosity. At the same time, crystals continuously grow on the periphery of the nanoparticulate aggregate, into a thin structural coating composed of intergrown coffin-shaped crystals. This dissolution-crystallization mechanism likely follows a well-known 'inside-out' Ostwald ripening process.<sup>48</sup>

A key benefit of the facile, one-step synthesis of hierarchical ZSM-5 is the establishment of a small ca. 15–25 nm diffusion length associated with the mesopore-intercalated nanocrystallites comprising the majority of the hierarchical structure. This small diffusion length, established within sub-micron (ca. 500 nm) zeolitic



**Scheme 1.** Proposed formation scheme and corresponding microscopy of structural evolution during the one-step, direct synthesis of the hierarchical ZSM-5 samples.

particles, combined with the remarkably low polycrystallinity, raises exciting potential for catalytic application of these materials in reaction systems (e.g., processing of bulky molecules) for which conventional microporous zeolites suffer from severe mass transport limitations.

In order to demonstrate the catalytic activity of the hierarchical zeolite catalysts, acid site concentrations on the external and internal

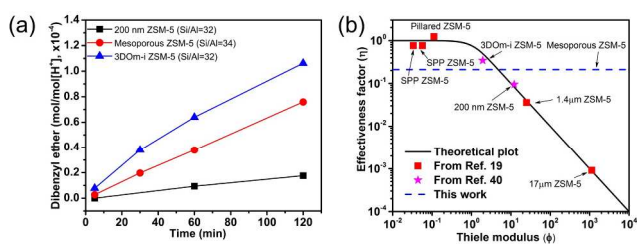


**Fig. 4.** (a) Production of dibenzyl ether per acid site as a function of reaction time, and (b) plot of effectiveness factor vs. Thiele modulus. The data of self-pillared pentasil (SPP), pillared MFI, 1.4 μm ZSM-5 and 17 μm ZSM-5 are from Ref.[19], and 3DOM-i ZSM-5 and 200nm ZSM-5 are from Ref.[40]. Detailed information is available in ESI.

surface of the catalysts were first evaluated. The decomposition of isopropylamine (IPA) into propylene and ammonia over Brønsted acid sites of the formed ZSM-5 catalysts showed the total acid sites of the hierarchical ZSM-5 (Si/Al = 30) to be around 0.53 mmol/g, indicating that most of the Al is incorporated within the framework. This is consistent with the FT-IR analysis of the sample using

adsorbed pyridine as a molecular probe (Fig. S13). The acid sites on the external surface were evaluated using a bulky amine, 2,4,6-trimethylpyridine (collidine), which is too large to enter the pore structure of ZSM-5. An acid site concentration of 0.039 mmol/g was obtained from the measurement, corresponding to 7.3% of the total acid sites. The value is similar to three-dimensionally ordered mesoporous imprinted (3DOM-i) ZSM-5 with a primary particle size (i.e., diffusion length scale) of 35 nm (9.1%),<sup>49</sup> but much higher than that associated with 200 nm ZSM-5 (2.1%),<sup>49</sup> indicating that the hierarchical ZSM-5 derived herein has a significantly higher fraction of acid sites on the external surface (Table S3).

The self-etherification reaction of benzyl alcohol in the presence of DTBP was chosen to test the catalytic performance of the hierarchical ZSM-5 catalysts. The added DTBP can poison the acid sites on the external surface of the catalysts, allowing the self-etherification reaction of benzyl alcohol to exclusively occur in the micropores of the synthesized ZSM-5. Fig. 4a reveals that the production of dibenzyl ether per acid site in the micropores for the synthesized hierarchical ZSM-5 catalyst was much higher than that of 200 nm ZSM-5, clearly indicating that the diffusion limitation can be greatly reduced by introduction of mesoporosity through the facile, direct synthesis process described herein. The effect of reducing mass transport limitations is comparable to that achieved with previously reported hierarchical ZSM-5 catalyst, e.g. 3DOM-i ZSM-5 (primary particle size is 35 nm)<sup>49</sup>, with a similar Si/Al, but has been accomplished here with a much simpler synthesis approach. Further comparison of the samples described in this work to other hierarchical ZSM-5 materials, reported in the literature and prepared in our previous studies,<sup>20, 49</sup> is provided in the context of a conventional effectiveness factor ( $\eta$ ) versus Thiele modulus ( $\phi$ ) plot in Fig. 4b. Given that the exact diffusion length (crystal size) of the hierarchical ZSM-5 catalyst synthesized in this study is unknown, the corresponding Thiele modulus ( $\phi$ ) is calculated from the point of intersection of the measured effectiveness factor ( $\eta$ ) with the theoretical curve. This diagram clearly reflects that the hierarchical

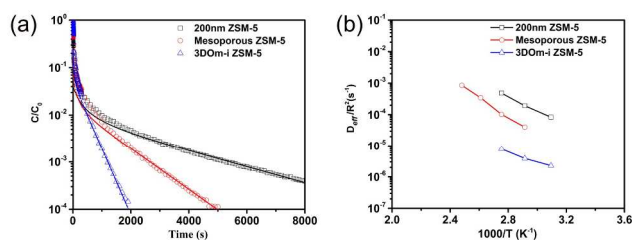


**Fig. 5.** (a) ZLC desorption curves for 200 nm ZSM-5 (Si/Al = 32), mesoporous ZSM-5 (Si/Al = 30) synthesized in this study and 3DOM-i ZSM-5 (Si/Al = 32) at 90 °C, (b) Summary of the effective diffusional time constants ( $D_{eff}/R^2$ ) obtained from ZLC analysis for the three zeolite samples.

ZSM-5 synthesized in this study is among the most effective ZSM-5 catalysts. The estimated diffusion length from the Thiele modulus for the hierarchical ZSM-5 catalyst is 25 nm, in good agreement with the TEM and SEM observations (Detailed information about the calculation is available in ESI and Table S4).

This small diffusion length achieved by a direct synthesis strategy in sub-micron particles is remarkable. The resulting enhanced mass transport of the hierarchical zeolites is also directly demonstrated by measuring the diffusion of cyclohexane in 200 nm ZSM-5, hierarchical ZSM-5, and 3DOM-i ZSM-5 by the zero length column

(ZLC) technique. Fig. 5a shows the experimental ZLC elution curves and fitted long-time analysis plots for these three samples at a temperature of 90 °C. Enhanced mass transport and diffusional time constants ( $D_{eff}/R^2$ ) (Fig. 5b,  $D_{eff}$  is the effective diffusivity of adsorbate in the crystal and  $R$  is the radius of the crystals) are observed in the case of the hierarchical ZSM-5 and 3DOM-i ZSM-5 samples in comparison to the 200 nm ZSM-5. These data provide strong evidence that the hierarchical ZSM-5 synthesized in this study can significantly facilitate the mass transport in the reactions involving bulky molecules without reliance on a complex, multi-step synthesis approach.

## Conclusions

In this work, we presented a facile, one-step method to synthesize hierarchical ZSM-5 catalysts without using any secondary templates that result in sub-micron catalyst particles with ca. 25 nm diffusion length, and, thereby, dramatically reduced mass transport limitation. The precursor particles formed in the initial stage and their assembly process play an important role for the formation of interstitial mesopores within the resulting structures. Based on experimental evidence, the unique hierarchical structure may evolve through a dissolution/recrystallization process, leading to an attractive broadening of the mesopore size distribution (3 nm to 15 nm) and concomitantly large mesopore volume, while maintaining significant microporosity associated with the crystalline nanoparticles. The synthesis method reported in this study provides a 'one-pot' approach to facile synthesis of hierarchical zeolites that requires no secondary template or post-synthetic treatment (e.g., steaming, dealumination) to derive intercalating mesoporosity. We have demonstrated the robustness, tunability, and ultimate versatility of this approach as it relates to key synthesis parameters such as Si/Al ratio, silica source, alkali concentration, and aging time. Taken together, these findings help establish key synthesis-structure relations for tuning properties of hierarchical ZSM-5 catalysts, and for generalizing this direct, one-step, and secondary-template-free approach to a wide range of zeolites and porous materials by precisely controlling the formation and assembly of precursor particles formed in the early stage of crystallization.

## Acknowledgements

This work was financially supported by the Catalysis Center for Energy Innovation (CCEI), an Energy Frontier Research Center funded by the US Dept. of Energy, Office of Science, and Office of Basic Energy Sciences under award number DE-SC0001004. C. L. thanks the supports from Chinese Scholarship Council (CSC, 201206150004) and Prof. Hongxia Xi at the South China University of Technology during his 2-year stay at UMass-Amherst.

## Notes and references

- M. Hartmann, *Angew. Chem. Int. Ed.*, 2004, 43, 5880-5882.
- J. Čejka and S. Mintova, *Catalysis Reviews*, 2007, 49, 457-509.
- J. Perez-Ramirez, C. H. Christensen, K. Egeblad, C. H. Christensen and J. C. Groen, *Chem. Soc. Rev.*, 2008, 37, 2530-2542.
- C. M. A. Parlett, K. Wilson and A. F. Lee, *Chem. Soc. Rev.*, 2013.
- Y. S. Tao, H. Kanoh, L. Abrams and K. Kaneko, *Chem. Rev.*, 2006, 106, 896-910.
- K. Egeblad, C. H. Christensen and M. Kustova, *Chem. Mater.*, 2008, 20, 946-960.
- K. Moller and T. Bein, *Chem. Soc. Rev.*, 2013, 42, 3689-3707.
- J. C. Groen, J. A. Moulijn and J. Perez-Ramirez, *J. Mater. Chem.*, 2006, 16, 2121-2131.
- J. C. Groen, W. D. Zhu, S. Brouwer, S. J. Huynink, F. Kapteijn, J. A. Moulijn and J. Perez-Ramirez, *J. Am. Chem. Soc.*, 2007, 129, 355-360.
- D. Verboekend and J. Perez-Ramirez, *Catal. Sci. Technol.*, 2011, 1, 879-890.
- K. S. Triantafyllidis, A. G. Vlessidis, L. Nalbandian and N. P. Evmiridis, *Microporous Mesoporous Mater.*, 2001, 47, 369-388.
- Z. T. Zhang, Y. Han, L. Zhu, R. W. Wang, Y. Yu, S. L. Qiu, D. Y. Zhao and F. S. Xiao, *Angew. Chem. Int. Ed.*, 2001, 40, 1258-1261.
- C. J. H. Jacobsen, C. Madsen, J. Houzvicka, I. Schmidt and A. Carlsson, *J. Am. Chem. Soc.*, 2000, 122, 7116-7117.
- I. Schmidt, C. Madsen and C. J. H. Jacobsen, *Inorg. Chem.*, 2000, 39, 2279-2283.
- H. Y. Chen, J. Wydra, X. Y. Zhang, P. S. Lee, Z. P. Wang, W. Fan and M. Tsapatsis, *J. Am. Chem. Soc.*, 2011, 133, 12390-12393.
- W. Fan, M. A. Snyder, S. Kumar, P. S. Lee, W. C. Yoo, A. V. McCormick, R. L. Penn, A. Stein and M. Tsapatsis, *Nat. Mater.*, 2008, 7, 984-991.
- M. Choi, H. S. Cho, R. Srivastava, C. Venkatesan, D. H. Choi and R. Ryoo, *Nat. Mater.*, 2006, 5, 718-723.
- M. Choi, K. Na, J. Kim, Y. Sakamoto, O. Terasaki and R. Ryoo, *Nature*, 2009, 461, 246-249.
- K. Na, C. Jo, J. Kim, K. Cho, J. Jung, Y. Seo, R. J. Messinger, B. F. Chmelka and R. Ryoo, *Science*, 2011, 333, 328-332.
- X. Y. Zhang, D. X. Liu, D. D. Xu, S. Asahina, K. A. Cychoz, K. V. Agrawal, Y. Al Wahedi, A. Bhan, S. Al Hashimi, O. Terasaki, M. Thommes and M. Tsapatsis, *Science*, 2012, 336, 1684-1687.
- Y. Fang, H. Hu and G. Chen, *Chem. Mater.*, 2008, 20, 1670-1672.
- A. A. Rownaghi and J. Hedlund, *Industrial & Engineering Chemistry Research*, 2011, 50, 11872-11878.
- A. A. Rownaghi, F. Rezaei and J. Hedlund, *Microporous Mesoporous Mater.*, 2012, 151, 26-33.
- T. Xue, L. Chen, Y. M. Wang and M.-Y. He, *Microporous Mesoporous Mater.*, 2012, 156, 97-105.
- K. Möller, B. Yilmaz, R. M. Jacubinas, U. Müller and T. Bein, *J. Am. Chem. Soc.*, 2011, 133, 5284-5295.
- T. M. Davis, T. O. Drews, H. Ramanan, C. He, J. S. Dong, H. Schnablegger, M. A. Katsoulakis, E. Kokkoli, A. V. McCormick, R. L. Penn and M. Tsapatsis, *Nat. Mater.*, 2006, 5, 400-408.
- P. de Moor, T. P. M. Beelen, B. U. Komanschek, L. W. Beck, P. Wagner, M. E. Davis and R. A. van Santen, *Chem.-Eur. J.*, 1999, 5, 2083-2088.
- W. Fan, M. Ogura, G. Sankar and T. Okubo, *Chem. Mater.*, 2007, 19, 1906-1917.
- V. Nikolakis, E. Kokkoli, M. Tirrell, M. Tsapatsis and D. G. Vlachos, *Chem. Mater.*, 2000, 12, 845-853.
- A. I. Lupulescu and J. D. Rimer, *Science*, 2014, 344, 729-732.
- Y. Liu, W. Z. Zhang and T. J. Pinnavaia, *Angew. Chem. Int. Ed.*, 2001, 40, 1255-1258.
- S. P. B. Kremer, C. E. A. Kirschhock, M. Tielen, F. Collignon, P. J. Grobet, P. A. Jacobs and J. A. Martens, *Adv. Funct. Mater.*, 2002, 12, 286-292.
- R. J. Gorte, *Catal. Lett.*, 1999, 62, 1-13.

34. O. Kresnawahjuesa, R. J. Gorte, D. de Oliveira and L. Y. Lau, *Catal. Lett.*, 2002, 82, 155-160.
35. A. R. Teixeira, C.-C. Chang, T. Coogan, R. Kendall, W. Fan and P. J. Dauenhauer, *J. Phys. Chem. C*, 2013, 117, 25545-25555.
36. C.-C. Chang, A. R. Teixeira, C. Li, P. J. Dauenhauer and W. Fan, *Langmuir*, 2013, 29, 13943-13950.
37. S. Brandani and D. M. Ruthven, *Adsorption*, 1996, 2, 133-143.
38. M. Eic and D. M. Ruthven, *Zeolites*, 1988, 8, 40-45.
39. L. Tosheva and V. P. Valtchev, *Chem. Mater.*, 2005, 17, 2494-2513.
40. A. E. Persson, B. J. Schoeman, J. Sterte and J. E. Otterstedt, *Zeolites*, 1995, 15, 611-619.
41. R. de Ruiter, J. C. Jansen and H. van Bekkum, *Zeolites*, 1992, 12, 56-62.
42. D. D. Kragten, J. M. Fedeyko, K. R. Sawant, J. D. Rimer, D. G. Vlachos, R. F. Lobo and M. Tsapatsis, *J. Phys. Chem. B*, 2003, 107, 10006-10016.
43. C. E. A. Kirschhock, R. Ravishankar, F. Verspeurt, P. J. Grobet, P. A. Jacobs and J. A. Martens, *J. Phys. Chem. B*, 1999, 103, 4965-4971.
44. N. D. Hould, S. Kumar, M. Tsapatsis, V. Nikolakis and R. F. Lobo, *Langmuir*, 2010, 26, 1260-1270.
45. J. M. Fedeyko, J. D. Rimer, R. F. Lobo and D. G. Vlachos, *J. Phys. Chem. B*, 2004, 108, 12271-12275.
46. S. Kumar, Z. P. Wang, R. L. Penn and M. Tsapatsis, *J. Am. Chem. Soc.*, 2008, 130, 17284-17286.
47. N. D. Hould and R. F. Lobo, *Chem. Mater.*, 2008, 20, 5807-5815.
48. B. Wang, H. B. Wu, L. Zhang and X. W. Lou, *Angew. Chem. Int. Ed.*, 2013, 52, 4165-4168.
49. Z. Wang, P. Dornath, C.-C. Chang, H. Chen and W. Fan, *Microporous Mesoporous Mater.*, 2013, 181, 8-16.

Hierarchical ZSM-5 with a shell of stacked coffin-shaped crystals and a core of nanocrystal aggregates was synthesized by controlling the formation and self-assembly of zeolite precursors formed in the initial stage of crystallization. The formed hierarchical zeolite shows superior catalytic activity for reaction involving bulky molecules due to enhanced mass transport.

